NASA Technical Memorandum 89146

IN-SITU TECHNIQUE FOR CHECKING THE CALIBRATION OF PLATINUM RESISTANCE THERMOMETERS

KAMRAN DARYABEIGI AND LAWRENCE A. DILLON-TOWNES

MAY 1987

National Aeronautics and Space Administration

Langley Research Center
Hampton, Virginia 23665

In-Situ Technique for Checking the Calibration of Platinum Resistance Thermometers

Kamran Daryabeigi and Lawrence A. Dillon-Townes

Langley Research Center
Hampton, Virginia

SUMMARY

The applicability of the self-heating technique as an in-situ method for checking the calibration of platinum resistance thermometers (PRT's) located inside wind tunnels has been investigated. This technique is based on a steady-state measurement of resistance (temperature) increase versus joule heating of the PRT. Changes in the calibration of PRT's were theoretically related to detectable changes in the behavior of the self-heating curves generated by this technique. Self-heating tests were performed in order to evaluate the related uncertainties in this technique. It was found that the self-heating technique is not applicable to PRT's used in wind tunnel environments, mainly because of the fluctuation of flow variables during any wind tunnel testing. These fluctuations produce errors that are larger than the acceptable tolerances for the self-heating technique.

INTRODUCTION

The applicability of the self-heating technique for checking the calibration of platinum resistance thermometers has been investigated. This work was motivated by the need for a systematic in-situ method for determining when a PRT located inside a wind tunnel needs to be recalibrated.

PRT's are being used more extensively for stagnation temperature measurement in wind tunnels, specifically cryogenic wind tunnels, because of their high precision. The thermophysical properties of gaseous nitrogen around 90 K are strongly temperature dependent, thus requiring very precise temperature measurements (ref. 1).

The resistance-temperature relationship of platinum is well known and has been utilized for accurate thermometry (ref. 2). A PRT is constructed of platinum wire wound around a frame or embedded in cement. Ideally, the wire must be free to expand and contract without constraint from its supports. This so-called "strain-free" construction is utilized in standard platinum resistance thermometers (SPRT's) suitable for laboratory environments. PRT's for industrial application employ partially or totally supported resistance windings in order to protect the sensor from mechanical shock, thus the platinum wire is not free to expand or contract. Therefore, the resistance of the PRT is not only a function of temperature, but is also related to the strain that results from the differential expansion of platinum wire and its supports. The wire may also be strained by vibration, thermal, or mechanical shocks. These strain effects could cause changes in the calibration of a PRT. The purpose of this investigation has been to determine the applicability of the self-heating technique as a means for checking the calibration of PRT's in order to determine when the changes in the calibration of a PRT are sufficient to require recalibration.

The self-heating technique has been implemented by Kerlin, et al., (ref. 3) for detecting changes in the response characteristics of degraded PRT's. This method is based on a steady-state measurement of resistance (temperature) increase versus joule heating in the sensing element. Changes in the slope of the resistance versus joule heating curve, the self-heating curve, have been related to changes in the overall heat transfer coefficient of PRT's, and therefore, related to changes in the response characteristics of the sensors (ref. 3). In this investigation, an attempt has been made to relate changes in the behavior of the self-heating curve to changes in the calibration of PRT's.

LIST OF SYMBOLS

A, B, C	calibration constants
E	error
h	convective heat transfer coefficient
K	Kelvin
k	thermal conductivity
ι	length
q	joule heating
R	resistance
R_o	ice-point resistance
Re	Reynolds number
r	radius
t	Platinum Resistance Thermometer temperature
t_∞	free-stream temperature
UA	overall heat transfer coefficient
V	voltage
α, β, δ	calibration constants
γ	slope of the self-heating curve
Δ	when preceding a symbol, signifies changes in that quantity
ω	y-intercept of the self heating curve

subscripts

s	precision calibration resistor

THEORETICAL ASPECTS OF THE SELF-HEATING TECHNIQUE

The resistance of a PRT is related to temperature in the temperature range from 90.18 K to 903.65 K according to Callendar-Van Dusen equation (ref. 4):

$$\frac{R}{R_o} = 1 + \alpha \left[t - \delta\left(\frac{t}{100} - 1\right)\left(\frac{t}{100}\right) - \beta\left(\frac{t}{100} - 1\right)\left(\frac{t}{100}\right)^3\right] \qquad (1)$$

R_o, α, β, and δ are constants determined by calibration at the freezing point of water, the boiling point of water, the boiling point of oxygen, and the freezing point of zinc, respectively. β is equal to zero for temperatures above 273.15 K. This calibration procedure and interpolation equation are in accordance with the International Practical Temperature Scale of 1948 (ref. 4), IPTS-48, which is different from the more recent, accurate, and complicated calibration procedure of IPTS-68 (ref. 5). The variation of temperature difference between temperatures defined on IPTS-68 and IPTS-48 for the temperature range 90 K to 330 K has a maximum value of 0.034 K (ref. 5). For the precision needed in this study, IPTS-48 formulation provides adequate accuracy, and is much simpler to use. Furthermore, industrial PRT's are not capable of producing the precision and resolution

specificed by IPTS-68.

Equation 1 can be transformed into a simpler form:

$$\frac{R}{R_o} = 1 + At + Bt^2 + Ct^3 \left(\frac{t}{100} - 1\right) \tag{2}$$

where:

$$A = \alpha\left(1 + \frac{\delta}{100}\right) \tag{2.1}$$

$$B = -10^{-4}\ \alpha\delta \tag{2.2}$$

$$C = -10^{-6}\ \alpha\beta \tag{2.3}$$

The sensitivity of a PRT is given by the first derivative of resistance with respect to temperature:

$$\frac{dR}{dt} = R_o\ [A + 2Bt + Ct^2\ (\frac{t}{25} - 3)] \tag{3}$$

Four PRT's have been used for the theoretical and experimental considerations throughout this study. These PRT's are representative of the PRT's used for the stagnation temperature measurement in the National Transonic Facility. The listing of these PRT's and their corresponding calibration data are provided in Table 1. The variation of resistance, sensitivity, and the rate of change of sensitivity with temperature (second derivative of resistance with respect to temperature) for PRT #1 is shown in figure 1. The resistance has been nondimensionalized with respect to the ice-point resistance, R_o, the resistance at the freezing point of water, while the sensitivity, and the rate of change of sensitivity have been nondimensionalized with respect to their corresponding values at 90 K. It can be seen from this figure that the sensitivity of a PRT increases with decreasing temperature.

Self-Heating Curve

The steady-state relationship between the sensor's temperature and joule heating generated in the sensor is:

$$q = UA\ (t - t_\infty) \tag{4}$$

When the PRT is operated with a one milliamp current which is the normal operating current of PRT's, the amount of heat generation in the sensor is negligible, thus yielding a negligible temperature difference between the sensor and its surroundings. Combining equations 2 and 4 yields the relationship between the resistance of the sensor and the joule heating, the so-called "self-heating" curve:

$$\frac{R}{R_o} = 1 + At_\infty + Bt_\infty^2 + Ct_\infty^3 \left(\frac{t_\infty}{100} - 1\right) + \left(\frac{q}{UA}\right)\ [A + 2Bt_\infty + Ct_\infty^2\ (\frac{t_\infty}{25} - 3)]$$

$$+ \left(\frac{q}{UA}\right)^2\ [B + 3Ct_\infty\ (\frac{t_\infty}{50} - 1)] + \left(\frac{q}{UA}\right)^3\ C(\frac{t_\infty}{25} - 1) + \left(\frac{q}{UA}\right)^4\ \frac{C}{100} \tag{5}$$

Changing the current supplied to a PRT results in different resistances and joule heatings. Plotting the resistance versus the heat generation constitutes the self-heating curve. If the PRT is operated with currents below 100 milliamps, the second and higher order heat generation terms in equation 5 are negligible. Therefore, a linear relationship between resistance and heat generation results:

$$\frac{R}{R_o} = 1 + At_\infty + Bt_\infty^2 + Ct_\infty^3 \left(\frac{t_\infty}{100} - 1\right) + \left(\frac{q}{UA}\right) \left[A + 2Bt_\infty + Ct_\infty^2 \left(\frac{t_\infty}{25} - 3\right)\right] \quad (6)$$

The validity of this approximation has been checked experimentally and will be described subsequently. The slope (γ) and y-intercept (ω)of the self-heating curve are:

$$\gamma = \left(\frac{R_o}{UA}\right) \left[A + 2Bt_\infty + Ct_\infty^2 \left(\frac{t_\infty}{25} - 3\right)\right] \quad (7)$$

$$\omega = R_o \left[1 + At_\infty + Bt_\infty^2 + Ct_\infty^3 \left(\frac{t_\infty}{100} - 1\right)\right] \quad (8)$$

Comparing the slope and y-intercept of the self-heating curve with equations 2 and 4 shows that the slope is basically the sensitivity of PRT divided by the overall heat transfer coefficient, and the y-intercept is the resistance of PRT as the current supplied to the PRT approaches zero.

Changes in the Self Heating Curve

The slope of a PRT subject to self-heating tests in a wind tunnel under similar flow conditions -- i.e., same temperature, pressure, velocity, and other heat transfer variables -- can change due to the following reasons:

1. Change of the overall heat transfer coefficient due to sensor degradation. Some of the different means of sensor degradation are (ref. 6): surface deposit build-ups, cracking of sensor internal materials, or redistribution of filler powders used in some sensors.

2. Change of the calibration constants of the PRT caused by straining effects. Kerlin, et al. (ref. 3) have proposed relating changes in the slope of the self-heating curve to changes in the overall heat transfer coefficient in an effort to predict changes in the response characteristics of PRT's.

In this investigation the relationship between the change in calibration constants and the change in the slope and y-intercept of the self-heating curves was examined. The changes in the slope and y-intercept of a PRT whose calibration constants have changed by ΔA, ΔB, ΔC, and ΔR_o can be calculated as follows (See Appendix A):

$$\frac{\Delta\gamma}{\gamma} = \left(1 + \frac{\Delta R_o}{R_o}\right) \frac{\Delta A + 2\Delta Bt_\infty + \Delta Ct_\infty^2 \left(\frac{t_\infty}{25} - 3\right)}{A + 2Bt_\infty + Ct_\infty^2 \left(\frac{t_\infty}{25} - 3\right)} + \frac{\Delta R_o}{R_o} \quad (9)$$

$$\frac{\Delta\omega}{\omega} = \left(1 + \frac{\Delta R_o}{R_o}\right) \frac{\Delta A t_\infty + \Delta B t_\infty^2 + \Delta C t_\infty^3 \left(\frac{t_\infty}{100} - 1\right)}{1 + A t_\infty + B t_\infty^2 + C t_\infty^3 \left(\frac{t_\infty}{100} - 1\right)} + \frac{\Delta R_o}{R_o} \tag{10}$$

The corresponding temperature error caused by using the original calibration constants instead of the modified ones would be obtained by:

$$\Delta t = \Theta - t \tag{11}$$

where t and Θ are the solutions to equation 2 using the original and the modified calibration constants, respectively. In an actual self-heating test the measured changes in slope and y-intercept can be related to temperature error through the following approximate formula (Appendix A):

$$\Delta t = \frac{1}{R_o X} (\Delta\omega + q\,\Delta\gamma) \tag{12}$$

where:

$$X = A + 2Bt_\infty + Ct_\infty^2 \left(\frac{t_\infty}{25} - 3\right) + \left(\frac{q}{UA}\right) \left[2B + 3Ct_\infty\left(\frac{t_\infty}{25} - 2\right)\right] + 3C\left(\frac{q}{UA}\right)^2 \left(\frac{t_\infty}{25} - 1\right) + \frac{C}{25}\left(\frac{q}{UA}\right)^3 \tag{13}$$

Typical changes in calibration constants of PRT's used at the NASA Langley Research Center are listed in table 2, and were used to study the variation in the behavior of the self-heating curve. The first set of calibration changes represents the average value of calibration change of SPRT's while the remaining sets are representative of industrial PRT's. The calibration data that were used in calculating calibration change number 8 in this table are presented in Appendix B. The variation of change in slope and y-intercept with temperature for PRT #3, subject to calibration change number 9 in table 2, is presented in figure 2. The variation of the corresponding temperature error is shown in figure 3.

The slope of the self-heating curve is the sensitivity of the PRT divided by the overall heat transfer coefficient. Neglecting the variation of the overall heat transfer coefficient with temperature, it can be concluded from figure 1 that the slope's sensitivity increases with decreasing temperature. Therefore, all of the subsequent analysis will be restricted to the case of free-stream temperature of 90 K, where the slope and y-intercept have the maximum sensitivity for the temperature range of interest in this study.

Table 3 presents the changes in slope, y-intercept, and the corresponding temperature error for PRT's #1 and 3 for a free-stream temperature of 90 K. These changes are due to shifts in calibration constants presented in table 2. The most significant detectable changes in the behavior of the self-heating curve occur at calibration changes number 8 and 9. Therefore, to study the effect of temperature error on the behavior of the self-heating curve, hypothetical calibration changes (table 4) covering the range between calibration changes number 8 and 9 were considered. Table 5 shows the corresponding changes in slope, y-intercept, and temperature error. It can be seen that for PRT #3, with an ice-point resistance of 100 ohms, a change in slope of about 3 percent would be equivalent to a temperature error of 0.5 K at 90 K. For PRT #1, with an ice-point resistance of 1000 ohms, a

change in slope of about 1 percent would be equivalent to a temperature error of 0.5 K at 90 K. Therefore, based on the result of this analysis it seems possible to employ the self-heating technique to detect changes in the calibration of PRT's. A one to three percent change in the slope of the self-heating curve would indicate that a temperature error of about 0.5 K would result at a free-stream temperature of 90 K if the original PRT calibration data are used. The success of the self-heating technique will depend upon the accuracy with which the self-heating data could be generated as well as the repeatability of test conditions for the self-heating tests.

EXPERIMENTAL INVESTIGATION

An experimental investigation was performed to evaluate the applicability of the self-heating technique in detecting changes in the calibration of PRT's. The issues that had to be addressed were:

1. Validation of the linearity of the self-heating curve (equation 2).

2. Determination of the precision of the calculated slope and y-intercept of the self-heating curve.

3. Examination of the effect of the non-repeatability of the wind tunnel flow variables on the self-heating curve.

4. Examination of the influence of the fluctuation of wind tunnel flow variables on the self-heating curve.

EXPERIMENTAL PROCEDURE

The experimental procedure consisted of performing self-heating tests in two wind tunnels:

1. Instrument Research Division's (IRD) low speed, open circuit flow velocity calibrator (ref. 7) for obtaining ambient temperature data and checking the experimental procedure.

2. 0.3 Meter Transonic Cryogenic Tunnel (TCT) (ref. 8) for obtaining data in the cryogenic range.

PRT #4 was tested in the test section of the IRD flow velocity calibrator, while PRT's #1 and 3 were tested in the settling chamber of the 0.3 Meter TCT.

The data acquisition system (fig. 4) used for this experimental investigation included: a Fluke model 8840A digital multimeter, a Racal-Dana series 1200 universal switch controller, two 100 ohm precision calibration resistors, two Fluke model 382A voltage/current calibrators, and a Hewlett Packard model 216 personal computer.

The PRT's were exposed to a self-heating test procedure. This procedure consisted of calculating the PRT resistance and joule heating for different amounts of current supplied to the PRT at different wind tunnel conditions. The direct current supplied to the PRT's was generally varied from 1 to 41 milliamps in increments of 10 milliamps. The resistances of the PRT's were determined using the

potentiometric method (ref. 9). This method is based on the determination of the ratio of the voltage drops across the prt sensor and a precision calibration resistor that are connected in series. The resistance value of the PRT was obtained from:

$$R = R_s \frac{V}{V_s} \tag{14}$$

where R_s and V_s represent the resistance and voltage across the precision calibration resistor. The amount of joule heating was calculated according to:

$$q = \frac{V\ V_s}{R_s} \tag{15}$$

The obtained resistance and heat generation data were curve fitted using a least-square method.

EXPERIMENTAL RESULTS

The results of the self-heating tests for PRT #4 used in the IRD flow velocity calibrator are presented in table 6. The flow conditions, temperature and Reynolds number, the corresponding slope and y-intercept of the self-heating curves, as well as the standard deviation of the linear curve fits are presented. The results of the self-heating tests for PRT's #1 and 3 in the 0.3 Meter TCT are presented in tables 7 and 8, respectively. Figure 5 shows the self-heating curve for PRT #3 which is typical of all PRT's and test conditions.

The variation of the y-intercepts of the three tested PRT's with free-stream temperature are generally in accordance with the theory, equation 8, as seen from tables 6, 7, and 8. That is the y-intercept increases as the temperature increases. The only exception is the second set of data in table 8 were the y-intercept has decreased with increasing temperature. This anomaly is most likely due to experimental error.

The behavior of the slopes as given in tables 6, 7, and 8 is more complicated to predict, because the slope is dependent upon flow variables such as temperature and Reynolds number. As seen from equation 7 the slope is the product of the reciprocal of the overall heat transfer coefficient and the sensitivity of the prt. The overall heat transfer coefficient is also a function of the same flow variables, while the sensitivity is a function of temperature only. In order to understand the variation of slope with flow variables, the variation of the overall heat transfer coefficient was studied.

The overall heat transfer coefficient given in equation 7 is related to flow variables according to (ref. 10):

$$\frac{1}{UA} = \sum_{i=1}^{n} \frac{\ln\left(\frac{r_{i+1}}{r_i}\right)}{2\pi\ k_i\ l} + \frac{1}{2\pi r_o\ h\ l} \tag{16}$$

where the first term represents the combined conductive heat transfer across the different layers of the PRT from the sensing wire to the outside surface. The second term represents the convective heat transfer resistance from the PRT to the

free stream. If the variation of the thermal conductivity of the PRT layers with temperature is neglected - an assumption valid for small temperature changes - equation 16 can be transformed to:

$$\frac{1}{UA} = C_1 + \frac{C_2}{h} \tag{17}$$

where C_1 and C_2 are constants. The convective heat transfer coefficient can be related to Reynolds number according to:

$$h = C_3 \, Re^n \tag{18}$$

where n is a constant depending upon the Reynolds number, and can be obtained from different correlations for convective heat transfer to cylinders (ref. 10). Substituting for convective heat transfer coefficient from equation 18 into equation 17 yields:

$$\frac{1}{UA} = C_1 + C_4 \, Re^{-n} \tag{19}$$

This equation provides the variation of the overall heat transfer coefficient with Reynolds number. It should be noted that the constants C_1 and C_4 are temperature dependent, but can be considered as constant because the variation of temperature throughout each of the IRD flow velocity calibrator and 0.3 Meter TCT experiments was less than 10 K. The experimental data for each of the PRT's were curve fitted in order to obtain the constants C_1 and C_4, which were then used to estimate the overall heat transfer coefficients for different test conditions. These estimated overall heat transfer coefficients were used in conjunction with the corresponding free-stream temperature measurements to calculate slopes according to equation 7. These predicted slopes are also listed in tables 6, 7, and 8. Although these predicted slopes are approximate values, they can provide an indication of how the slope should vary with temperature and Reynolds number for the given test conditions.

Comparing the predicted and calculated values of slope for the three PRT's, it can be seen that the experimentally determined slopes do not always follow the pattern indicated by the predicted values. Some erratic behavior can be observed in the data for all the PRT's.

These erratic behaviors in the y-intercept and slope data could be related to uncertainties and errors present in the experiments. The errors and uncertainties are comprised of three factors: the inherent uncertainty in instrumentation, the error involved in curve fitting the experimental data, and the fluctuation of flow variables during each set of self-heating tests. Each of these factors will be discussed subsequently.

The instrumentaion error is related to the determination of the resistance and joule heating of the PRT according to equations 14 and 15. The errors in the calculated values of PRT resistance and joule heating were estimated using the root-sum-square method (ref. 11):

$$E_R = \left((\Delta V \frac{\partial R}{\partial V})^2 + (\Delta V_s \frac{\partial R}{\partial V_s})^2 \right)^{0.5} \tag{20}$$

$$E_q = \left((\Delta V \frac{\partial R}{\partial V})^2 + (\Delta V_s \frac{\partial q_s}{\partial V_s})^2 \right)^{0.5} \tag{21}$$

where ΔV and ΔV_s represent the uncertainties in the measured voltages across the sensor and the standard resistor, respectively, and were estimated using the

multimeter manufacturer's specified uncertainties (ref. 12). The maximum error for the calculated values of resistance and joule heating due to instrumentation error was estimated to be 0.03 percent of the readings.

The resistance and joule heating data for each set of experiments were curve fitted to a linear relationship. The maximum average standard deviation of the PRT resistances obtained by linear curve fit of the experimental data was 0.18 percent.

Fluctuation of flow variables such as temperature and Reynolds number could also contribute to error in the self-heating tests. In wind tunnel testing the flow variables can not be maintained at fixed values and undergo fluctuations. Fluctuations of 0.5 K in free-stream temperature and 0.5 million in test section's Reynolds number were sometimes observed in the 0.3 Meter TCT data. These Reynolds number fluctuations correspond to a 2000-5000 variation in the settling chamber's Reynolds number in this wind tunnel. These fluctuations were even observable in the raw data of the self-heating tests. In a few instances it was observed that the resistance of the PRT would decrease with increasing current. This could only be related to an instantaneous decrease in free-stream temperature, and/or increase in the Reynolds number. Both possibilities would cause a decrease in the temperature of the sensor, thus causing a decrease in the resistance even though the current supplied to the sensor had increased. These fluctuating data would yield self-heating curves that would deviate significantly from the predicted behaviors. Most of the fluctuating data presented in tables 6, 7, and 8 correspond to erratic behavior due to temperature and Reynolds number fluctuations. Fluctuations of these flow variables would invalidate the self-heating technique.

Another source of error in the self-heating technique is the non-repeatability of flow variables during successive tests. The self-heating technique consists of generating the self-heating curve at a given set of flow variables, and then repeating the tests under the same flow conditions in order to compare the self-heating curves. Repeatability of flow variables during successive tests may not be achievable. Figure 6 shows the percent change in slope and y-intercept of a self-heating curve for PRT #3 due to a ±1 K variation about a selected free-stream temperature for different temperatures. The maximum discrepancy in the slope and y-intercept was 0.07 percent and 1.80 percent, respectively. The percent change in the slope of a self-heating curve for the PRT's used in the 0.3 Meter TCT due to a ±1 percent variation of the Reynolds number for different Reynolds numbers is presented in table 9. Both the test section Reynolds numbers and the settling chamber Reynolds numbers are tabulated. It can be seen that the average corresponding errrors for PRT's #1 and 3 are ±0.77 percent and ±0.27 percent, respectively.

CONCLUSION

The applicability of the self-heating technique as an in-situ method for checking the calibration of platinum resistance thermometers has been investigated.

Based on the results of this investigation it can be concluded that the self-heating technique cannot be applied for in-situ testing of the calibration of PRT's used in wind tunnel environments. The fluctuation of flow variables in a wind tunnel invalidate this technique. Furthermore, the possible non-repeatability of flow conditions for possible comparison of self-heating data also introduce significant uncertainties in the method to render it useless. The self-heating test method appears to be only applicable in totally controlled environments such as

liquid baths where the fluctuation of parameters can be made negligible and repeatability of test conditions can be achieved.

One possible way to circumvent the problems associated with the fluctuation of flow variables during the self-heating tests would be to gather a large sample of data in order to be able to statistically eliminate some of the erratic behavior. However, the cost involved in gathering a large sample of wind tunnel data, and the fact that such data might still not produce good results render this technique undesirable.

Langley Research Center
National Aeronautics and Space Administration
Hampton, VA 23665-5225
April 1987

References

1. Goodyear, M. J., and Kilgore, R. A.: High-Reynolds-Number Cryogenic Wind Tunnel. AIAA Journal, vol. 11, 1973, pp. 613-619.

2. Clark, J. A.: Temperature Measurement in Cryogenics. Ch. 4, Measurements in Heat Transfer, 2nd ed., edited by E. R. G. Eckert and R. J. Goldstein, Hemisphere Publishing Corporation, 1976.

3. Kerlin, T. W., Miller, L. F., and Hashemian, H. M.: In-Situ Response Time Testing of Platinum Resistance Thermometers. ISA Transactions, vol. 17, 1978, pp. 71-88.

4. Stimson, H. F.: The Text Revision of the International Temperature Scale of 1948. Temperature, Its Measurement and Control in Science and Industry, Part I, edited by F. G. Brickweddo, Reinhold Publishing Corporation, vol. 3, 1962, pp. 59-66.

5. The International Practical Temperature Scale of 1968, Amended Edition of 1975. Metrologia, vol. 12, 1976, pp. 7-17.

6. Kerlin, T. W., Hashemian, H. M., and Petersen, K. M.: Time Response of Temperature Sensors. ISA Transactions, vol. 20, 1981, pp. 65-77.

7. Daryabeigi, K.: Convective Heat Transfer from Circular Cylinders Located Within Perforated Cylindrical Shrouds. M. S. Thesis, Old Dominion University, 1986.

8. Ray, E. J., Kilgore, R. A., Adcock, J. B., and Davenport, E. E.: Analysis of Validation Tests of the Langley Pilot Transonic Cryogenic Tunnel. Journal of Aircraft, vol. 12, 1975, pp. 539-544.

9. Riddle, J. L., Furukawa, G. T., and Plumb, H. H.: Platinum Resistance Thermometry. Ch. 2, Measurements in Heat Transfer, 2nd ed., edited by E. R. G. Eckert and R. J. Goldstein, Hemisphere Publishing Corporation, 1976.

10. Kreith, F., and Black, W. Z., Basic Heat Transfer, Harper & Row Publishers, 1980.

11. Doebelin, E. O.: Generalized Performance Characteristics of Instruments. Ch. 3, Measurement Systems, Application and Design, 3rd ed., McGraw-Hill Book Company, 1983.

12. 8840 Multimeter Instruction Manual, John Fluke Manufacturing Company, 1984.

TABLE I.- LISTING OF THE PRT'S USED IN THE ANALYSIS

PRT No. Manufacturer Model Serial No.	1 Rosemount 134-RL 19399	2 Rosemount 134-RL 19398	3 Hy-Cal RTS-54-B-100 313	4 Hy-Cal RTS-32A-100-B12 35
Wind Tunnel Used For Testing	0.3 Meter TCT	———	0.3 Meter TCT	IRD Flow Velocity Calibrator
A	3.9790266 E-3	3.9788334 E-3	3.9760648 E-3	3.9165111 E-3
B	-5.8336260 E-7	-5.8487864 E-7	-5.9430633 E-7	-5.7594465 E-7
C	-4.1607280 E-10	-4.5030086 E-10	-3.6995277 E-10	-4.7488331 E-10
R_o	1000.130	1000.672	99.897	99.870

TABLE II.- TYPICAL CHANGES IN THE CALIBRATION CONSTANTS OF PRT'S USED AT NASA LANGLEY RESEARCH CENTER

Calibration Change No.	$\frac{\Delta A}{A}$	$\frac{\Delta B}{B}$	$\frac{\Delta C}{C}$	$\frac{\Delta R_o}{R_o}$
1	7.76E-6	9.44E-5	-1.24E-3	-1.15E-5
2	2.64E-4	5.96E-3	-4.62E-2	-7.20E-5
3	5.38E-4	7.19E-3	-6.43E-2	1.42E-4
4	1.60E-4	3.86E-3	-2.22E-2	-1.30E-4
5	9.95E-5	5.71E-3	-1.21E-2	-5.50E-5
6	-9.44E-4	-1.23E-2	0.11	-6.20E-5
7	1.61E-3	5.17E-2	-1.85E-1	-1.60E-5
8	2.56E-3	8.12E-2	-2.69E-1	-6.89E-5
9	1.05E-2	0.196	-3.80	-1.55E-3

TABLE III.- CHANGES IN THE SELF-HEATING CURVE, AND THE CORRESPONDING TEMPERATURE ERROR OF PRT'S SUBJECT TO CHANGES IN CALIBRATION CONSTANTS LISTED IN TABLE II.

Calibration Change No.	PRT #1			PRT #3		
	$\frac{\Delta\omega}{\omega} \times 100$	$\frac{\Delta\gamma}{\gamma} \times 100$	Δt (K)	$\frac{\Delta\omega}{\omega} \times 100$	$\frac{\Delta\gamma}{\gamma} \times 100$	Δt (K)
1	-5.5E-4	-0.004	0.000	-9.7E-4	-0.004	-0.001
2	0.003	-0.107	0.002	-0.013	-0.090	-0.007
3	-0.013	-0.115	-0.008	-0.035	-0.091	-0.020
4	-0.026	-0.053	-0.015	-0.034	-0.045	-0.019
5	-0.045	-0.008	-0.025	-0.050	-0.003	-0.028
6	0.048	0.212	0.027	0.085	0.171	0.048
7	-0.348	-0.214	-0.196	-0.414	-0.142	-0.235
8	-0.624	-0.266	-0.351	-0.721	-0.160	-0.409
9	6.39	-10.8	3.605	5.090	-9.45	2.895

TABLE IV.- ADDITIONAL SETS OF CHANGE IN CALIBRATION CONSTANTS OF PRT'S

Calibration Change No.	$\frac{\Delta A}{A}$	$\frac{\Delta B}{B}$	$\frac{\Delta C}{C}$	$\frac{\Delta R_o}{R_o}$
A1	2.50E-3	8.00E-2	-3.00E-1	-7.00E-5
A2	3.75E-3	1.20E-1	-4.50E-1	-1.05E-4
A3	5.63E-3	1.80E-1	-6.75E-1	-1.58E-4
A4	8.44E-3	2.70E-1	-1.01	-2.37E-4
A5	1.27E-2	4.05E-1	-1.51	-3.55E-4
A6	1.90E-2	6.07E-1	-2.28	-5.31E-4

TABLE V.- CHANGES IN THE SELF-HEATING CURVE, AND THE CORRESPONDING TEMPERATURE ERROR FOR PRT'S SUBJECT TO CHANGES IN CALIBRATION CONSTANTS LISTED IN TABLE IV.

Calibration Change No.	PRT #1			PRT #3		
	$\frac{\Delta\omega}{\omega} \times 100$	$\frac{\Delta\gamma}{\gamma} \times 100$	Δt (K)	$\frac{\Delta\omega}{\omega} \times 100$	$\frac{\Delta\gamma}{\gamma} \times 100$	Δt (K)
A1	-0.50	-0.38	-0.284	-0.61	-0.26	-0.347
A2	-0.76	-0.57	-0.426	-0.92	-0.40	-0.521
A3	-1.13	-0.86	-0.640	-1.38	-0.59	-0.782
A4	-1.70	-1.28	-0.959	-2.06	-0.89	-1.172
A5	-2.55	-1.92	-1.438	-3.10	-1.33	-1.758
A6	-3.83	-2.89	-2.156	-4.64	-2.00	-2.635

TABLE VI.- RESULTS OF THE SELF-HEATING TESTS IN THE IRD FLOW VELOCITY CALIBRATOR

Test No.	Temperature (K)	Re	y-Intercept	Slope		Standard Deviation of Curve Fit
				Calculated	Predicted	
1	297.32	6.13E3	109.26	6.1099	6.462	6.20E-2%
2	297.34	9.19E3	109.29	6.0044	6.234	3.21E-2%
3	298.79	1.22E4	109.84	6.2627	6.104	3.24E-2%
4	299.15	1.53E4	109.97	6.0831	6.009	4.38E-2%

TABLE VII.- RESULTS OF THE SELF-HEATING TESTS FOR PRT #1 IN THE 0.3 METER TCT

Test No.	Temperature (K)	Re	y-Intercept	Slope		Standard Deviation of Curve Fit
				Calculated	Predicted	
1	99.13	2.85E5	284.70	15.94	15.44	7.34E-2%
2	99.21	2.98E5	282.87	13.71	14.94	4.5 E-2%
3	99.35	2.29E5	------	-----	-----	No Data Taken
4	99.74	2.14E5	287.29	18.10	19.25	1.04E-1%
5	103.89	3.53E5	305.02	13.31	13.09	8.95E-2%
6	109.21	3.44E5	328.25	11.45	13.29	7.27E-2%

TABLE VIII.- RESULTS OF THE SELF-HEATING TESTS FOR PRT #3 IN THE 0.3 METER TCT

Test No.	Temperature (K)	Re	y-Intercept	Slope		Standard Deviation of Curve Fit
				Calculated	Predicted	
1	99.13	2.85E5	28.333	7.61	7.54	1.51E-1%
2	99.21	2.98E5	28.478	7.53	7.45	3.14E-2%
3	99.35	2.29E5	28.582	6.60	8.03	1.18E-1%
4	99.74	2.14E5	28.638	8.38	8.21	1.76E-1%
5	103.89	3.53E5	30.405	5.84	7.12	4.11E-3%
6	109.21	3.44E5	32.581	7.41	7.14	9.10E-3%

TABLE IX.- CHANGE IN THE SLOPE OF THE SELF-HEATING CURVE CAUSED BY A ±1% VARIATION OF THE SETTLING CHAMBER'S REYNOLDS NUMBER IN THE 0.3 METER TCT

Settling Chamber's Reynolds No. Based on Sensor Diameter	Test Section's Reynolds No. Based on a One Foot Cord	Percent Change in Slope	
		PRT #3	PRT #1
2.20E5	60.0E6	0.31	0.77
3.00E5	80.0E6	0.27	0.77
3.50E5	99.0E6	0.24	0.76

APPENDIX A

CHANGES IN THE SELF-HEATING CURVE AND THE CORRESPONDING TEMPERATURE ERROR CAUSED BY CHANGE IN CALIBRATION

The slope and y-intercept of the self heating curve are given by:

$$\gamma = \frac{R_o}{UA} \left[A + 2Bt_\infty + Ct_\infty^2 \left(\frac{t_\infty}{25} - 3\right)\right] \tag{A.1}$$

$$\omega = R_o \left[1 + At_\infty + Bt_\infty^2 + Ct_\infty^3 \left(\frac{t_\infty}{100} - 1\right)\right] \tag{A.2}$$

If the calibration constants change by ΔA, ΔB, ΔC, and ΔR_o, such that the new calibration constants are:

$$A_1 = A + \Delta A \tag{A.3}$$

$$B_1 = B + \Delta B \tag{A.4}$$

$$C_1 = C + \Delta C \tag{A.5}$$

$$R_{o1} = R_o + \Delta R_o \tag{A.6}$$

the new slope and y-intercept of the self-heating curve become:

$$\gamma_1 = \frac{R_{o1}}{UA} \left[A_1 + 2B_1 t_\infty + C_1 t_\infty^2 \left(\frac{t_\infty}{25} - 3\right)\right] \tag{A.7}$$

$$\omega_1 = R_{o1} \left[1 + A_1 t_\infty + B_1 t_\infty^2 + C_1 t_\infty^3 \left(\frac{t_\infty}{100} - 1\right)\right] \tag{A.8}$$

The corresponding changes in the slope and y-intercept can be obtained by subtracting Equations A.1 and A.2 from A.7 and A.8, respectively:

$$\frac{\Delta\gamma}{\gamma} = \left(1 + \frac{\Delta R_o}{R_o}\right) \frac{\Delta A + 2\Delta Bt_\infty + \Delta Ct_\infty^2 \left(\frac{t_\infty}{25} - 3\right)}{A + 2Bt_\infty + Ct_\infty^2 \left(\frac{t_\infty}{25} - 3\right)} + \frac{\Delta R_o}{R_o} \tag{A.9}$$

$$\frac{\Delta\omega}{\omega} = \left(1 + \frac{\Delta R_o}{R_o}\right) \frac{\Delta At_\infty + \Delta Bt_\infty^2 + \Delta Ct_\infty^3 \left(\frac{t_\infty}{100} - 1\right)}{1 + At_\infty + Bt_\infty^2 + Ct_\infty^3 \left(\frac{t_\infty}{100} - 1\right)} + \frac{\Delta R_o}{R_o} \tag{A.10}$$

The resistance of a PRT is related to the joule heating according to:

$$R = \omega + \gamma q \tag{A.11}$$

The change in the resistance reading of a PRT at a given free-stream temperature caused by changes in the calibration constants can be obtained from:

$$\Delta R = \Delta\omega + q\,\Delta\gamma \tag{A.12}$$

This change in resistance can be converted to a change in the indicated temperature of the PRT according to the chain rule:

$$\Delta t = \Delta R \frac{dt}{dR} \tag{A.13}$$

Substituting for $\frac{dt}{dR}$ from equation 3 results in:

$$\Delta t = \frac{\Delta\omega + q\,\Delta\gamma}{R_o \left[A + 2Bt + Ct^2 \left(\frac{t}{25} - 3\right)\right]} \tag{A.14}$$

Substituting for the PRT temperature, t, from equation 4 results in:

$$\Delta t = \frac{\Delta\omega + q\,\Delta\gamma}{R_o X} \tag{A.15}$$

where X is provided in equation 13.

APPENDIX B

TYPICAL CHANGES IN CALIBRATION DATA

Calibration change No. 8 in table 2 corresponds to prt #4. The calibration data and the calculated changes in calibration constants are tabulated here:

Calibration Date	November 1983	November 1984
Calibration Constants		
A	3.9686854 E-3	3.9788334 E-3
B	-5.4096148 E-7	-5.8487864 E-7
C	-6.1612356 E-10	-4.5030086 E-10
R_o	1000.741	1000.672
Corresponding Change in Calibration Constants		
$\frac{\Delta A}{A}$	———	2.56 E-3
$\frac{\Delta B}{B}$	———	8.12 E-2
$\frac{\Delta C}{C}$	———	-2.69 E-1
$\frac{\Delta R_o}{R_o}$	———	-6.89 E-5

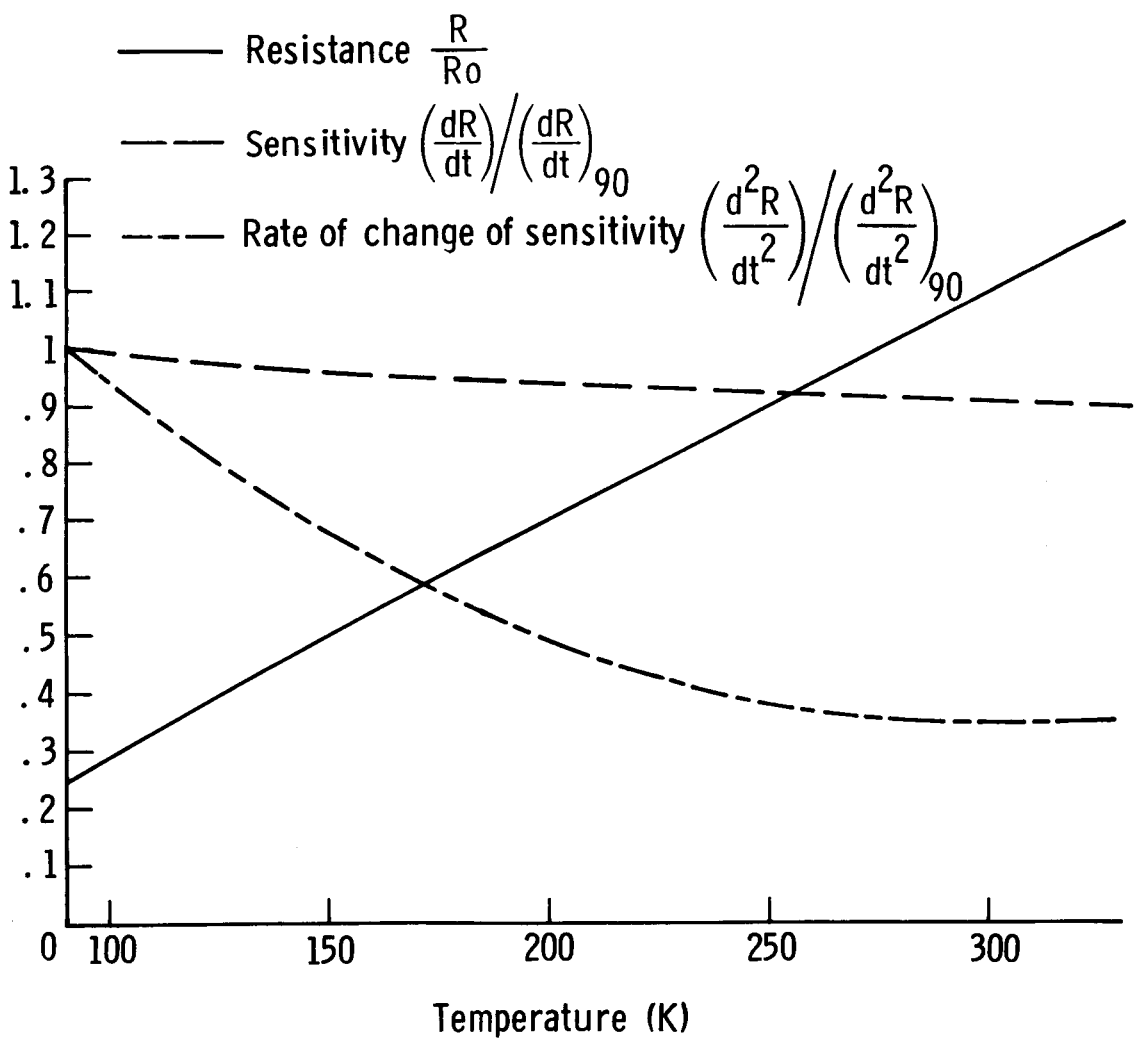

Figure 1.- Variation of PRT's resistance, sensitivity, and the rate of change of sensitivity with temperature.

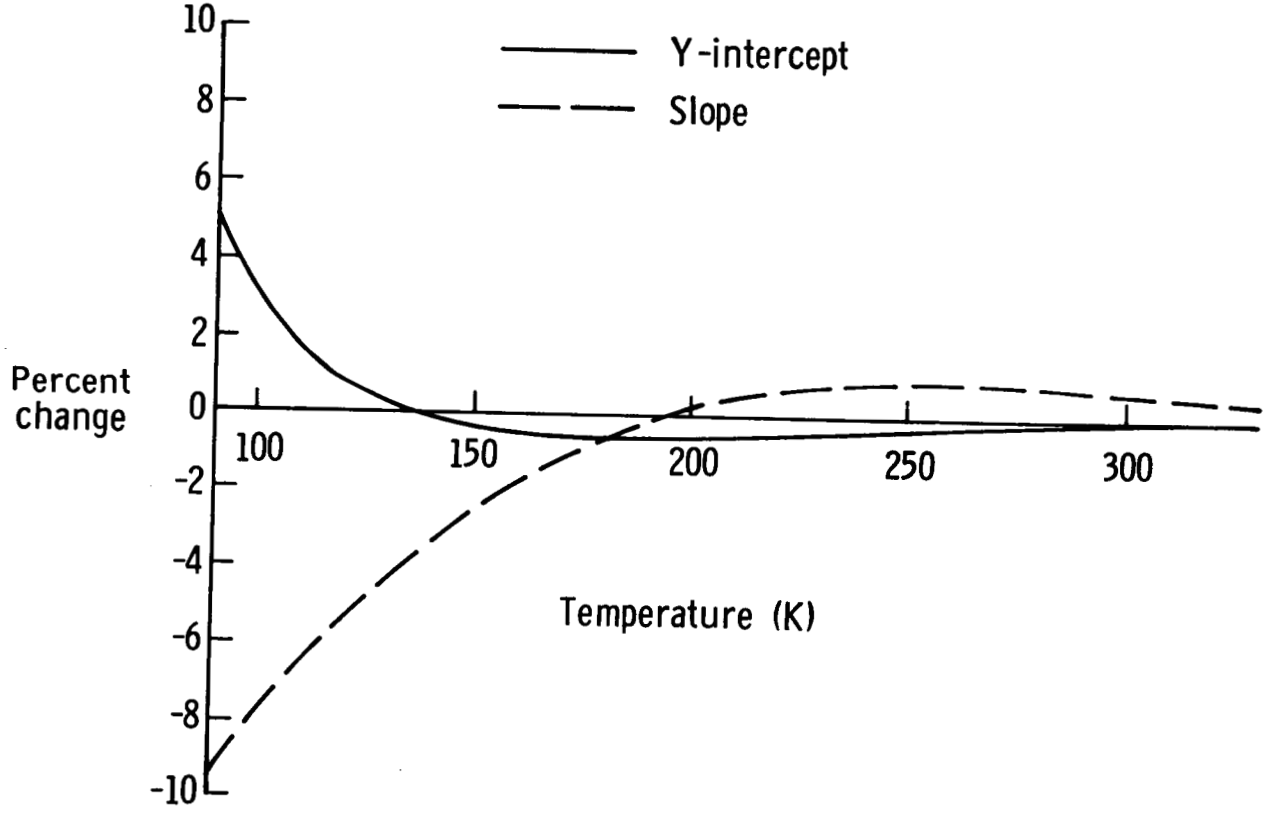

Figure 2.- Variation of change in slope and y-intercept with temperature caused by change in calibration No. 9 of PRT #3.

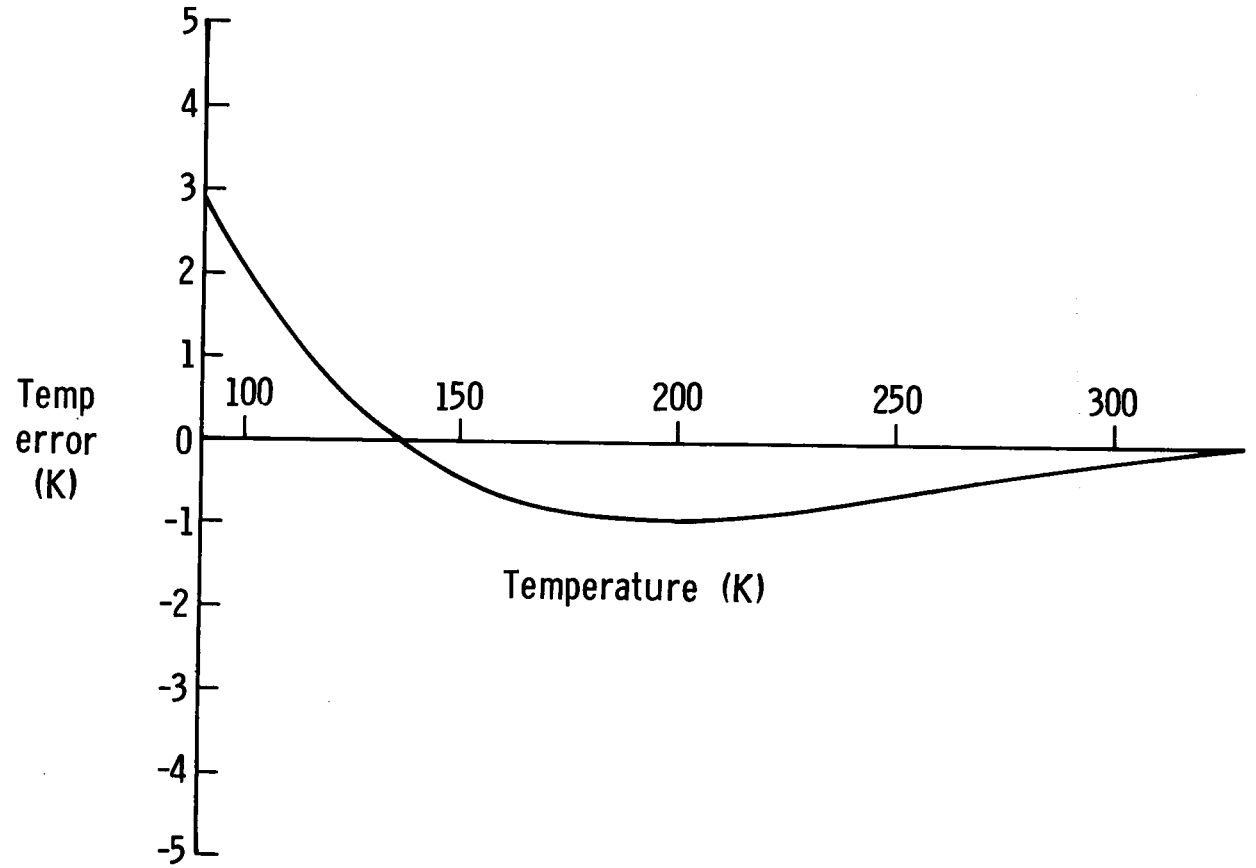

Figure 3.- Variation of temperature error with temperature caused by change in calibration No. 9 of PRT #3.

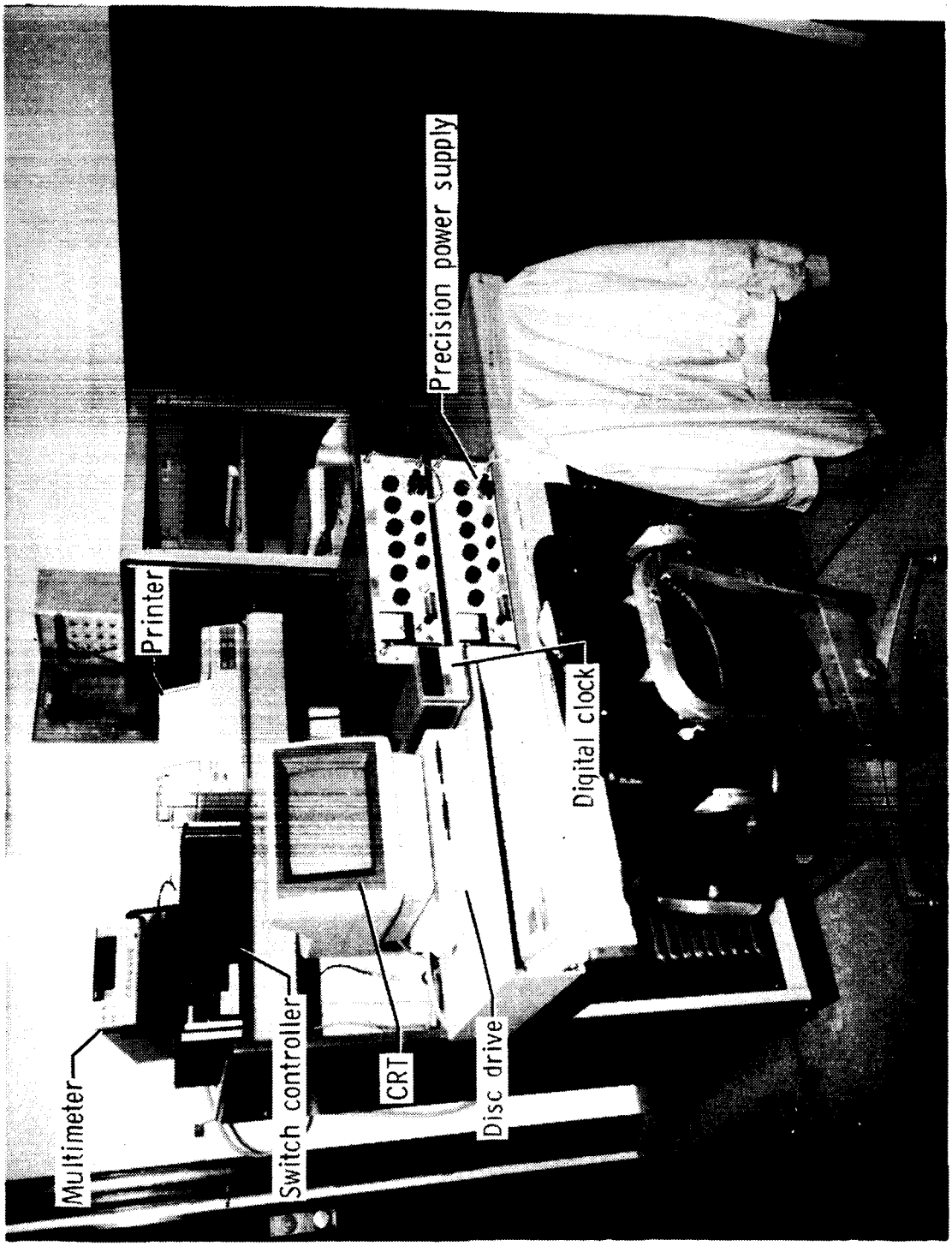

NASA
L-86-4186

Figure 4.- Experimental Set-Up

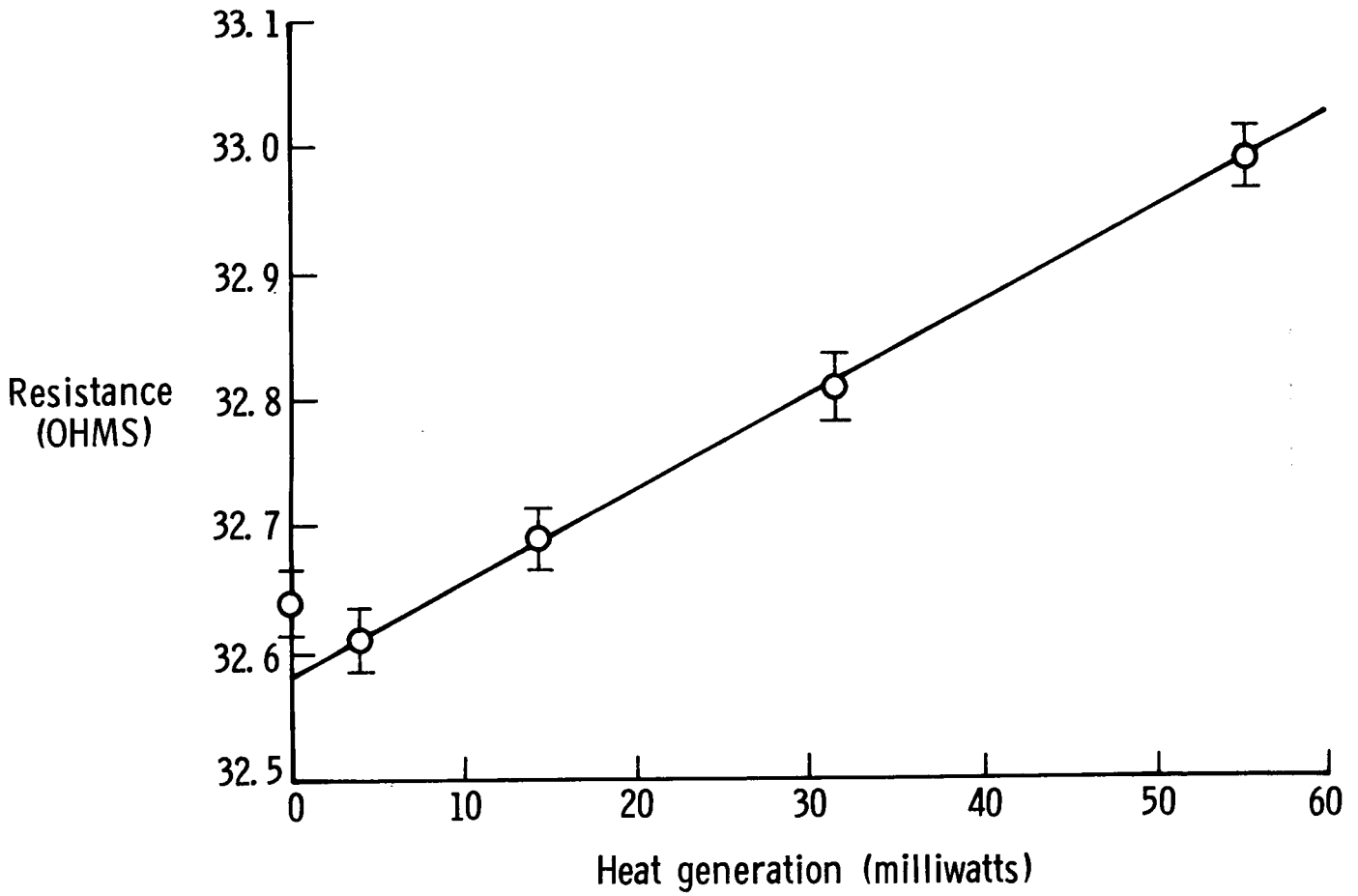

Figure 5.- A self-heating curve for 0.3 Meter TCT tests.

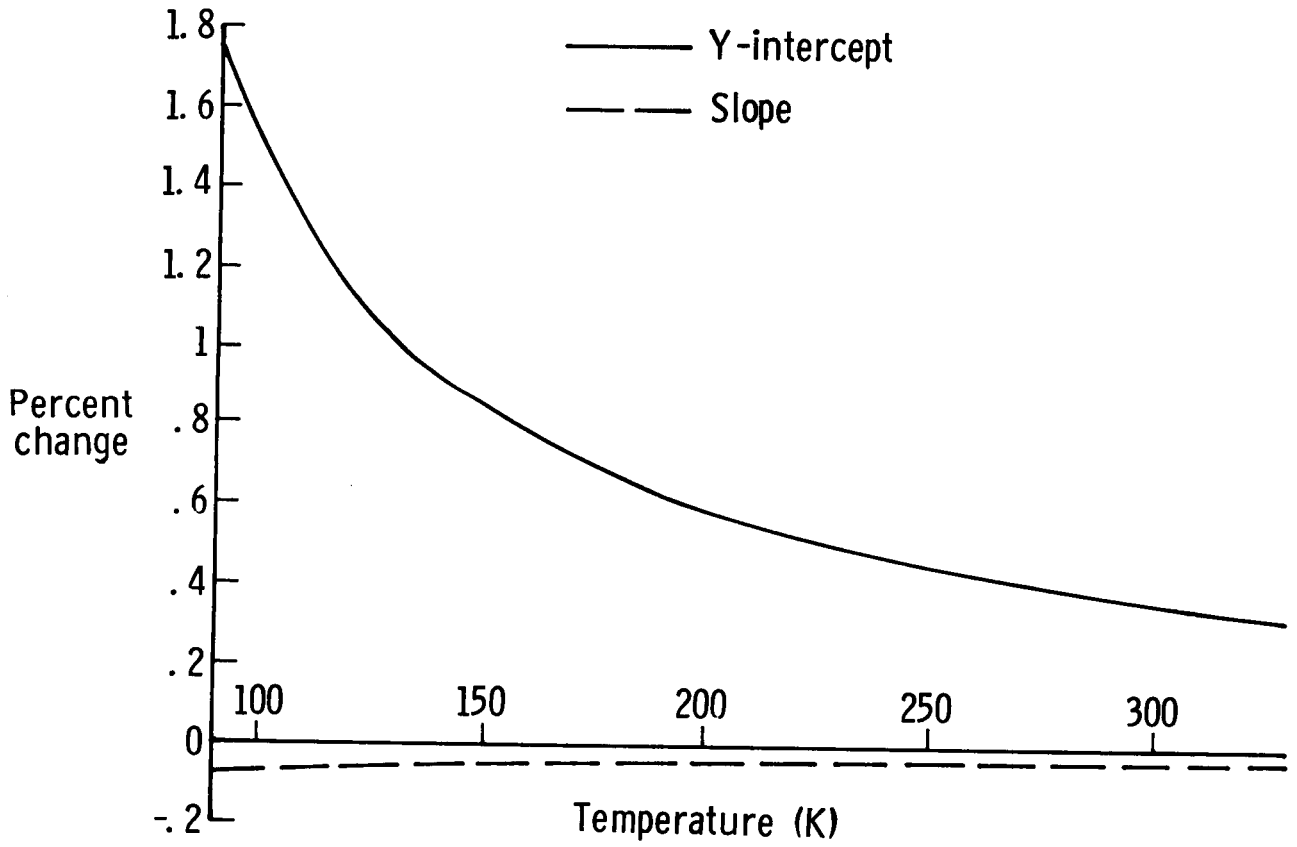

Figure 6.- Variation of change in slope and y-intercept with temperature due to ±1K temperature fluctuation for PRT #3.

Standard Bibliographic Page

1. Report No.	2. Government Accession No.	3. Recipient's Catalog No.
NASA TM-89146		

4. Title and Subtitle	5. Report Date
In-Situ Technique for Checking the Calibration of Platinum Resistance Thermometers	May 1987
	6. Performing Organization Code
7. Author(s)	8. Performing Organization Report No.
Kamran Daryabeigi and Lawrence A. Dillon-Townes	
9. Performing Organization Name and Address	10. Work Unit No.
NASA Langley Research Center Hampton, VA 23665-5225	506-61-01-05
	11. Contract or Grant No.
12. Sponsoring Agency Name and Address	13. Type of Report and Period Covered
National Aeronautics and Space Administration Washington, DC 20546	Technical Memorandum
	14. Sponsoring Agency Code

15. Supplementary Notes

16. Abstract

The applicability of the self-heating technique for checking the calibration of platinum resistance thermometers located inside wind tunnels was investigated. This technique is based on a steady state measurement of resistance increase versus joule heating. This method was found to be undesirable, mainly because of the fluctuations of flow variables during any wind tunnel testing.

17. Key Words (Suggested by Authors(s))	18. Distribution Statement
Resistance Thermometer Self-Heating Technique Calibration Check	Unclassified - Unlimited Subject Category 35

19. Security Classif.(of this report)	20. Security Classif.(of this page)	21. No. of Pages	22. Price
Unclassified	Unclassified	30	A03

For sale by the National Technical Information Service, Springfield, Virginia 22161

NASA Langley Form 63 (June 1985)